


## Article

# A Case Study of a Large Unstable Mass Stabilization: “El Portalet” Pass at the Central Spanish Pyrenees

Guillermo Cobos <sup>1,\*</sup>, Miguel Ángel Eguibar <sup>2</sup>, Francisco Javier Torrijo <sup>1,3</sup> and Julio Garzón-Roca <sup>4</sup>

<sup>1</sup> Department of Geological and Geotechnical Engineering, Universitat Politècnica de València, 46022 Valencia, Spain; meguibar@hma.upv.es

<sup>2</sup> Department of Hydraulic Engineering and Environment, Institute for Water and Environmental Engineering (IIAMA), Universitat Politècnica de València, 46022 Valencia, Spain; fratorec@trr.upv.es

<sup>3</sup> Research Centre PEGASO, Universitat Politècnica de València, 46022 Valencia, Spain

<sup>4</sup> Department of Geodynamics (GEODESPAL), Faculty of Geology, Complutense University of Madrid, 28040 Madrid, Spain; julgarzo@ucm.es

\* Correspondence: gcobosc@trr.upv.es

**Abstract:** This case study presents the engineering approach conducted for stabilizing a landslide that occurred at “El Portalet” Pass in the Central Spanish Pyrenees activated due to the construction of a parking lot. Unlike common slope stabilization cases, measures projected here were aimed at slowing and controlling the landslide, and not completely stopping the movement. This decision was taken due to the slow movement of the landslide and the large unstable mass involved. The degree of success of the stabilization measures was assessed by stability analyses and data obtained from different geotechnical investigations and satellite survey techniques such as GB-SAR and DinSAR conducted by different authors in the area under study. The water table was found to be a critical factor in the landslide’s stability, and the tendency of the unstable slope for null movement (total stability) was related to the water table lowering process, which needs more than 10 years to occur due to regional and climatic issues. Results showed a good performance of the stabilization measures to control the landslide, demonstrating the effectiveness of the approach followed, and which became an example of a good response to the classical engineering duality cost–safety.

**Keywords:** landslide; safety factor; Central Spanish Pyrenees; soft rocks; stabilization measures



**Citation:** Cobos, G.; Eguibar, M.Á.; Torrijo, F.J.; Garzón-Roca, J. A Case Study of a Large Unstable Mass Stabilization: “El Portalet” Pass at the Central Spanish Pyrenees. *Appl. Sci.* **2021**, *11*, 7176. <https://doi.org/10.3390/app11167176>

Academic Editors: Ricardo Castedo, Miguel Llorente Isidro and David Moncoulon

Received: 2 July 2021

Accepted: 2 August 2021

Published: 4 August 2021

**Publisher’s Note:** MDPI stays neutral with regard to jurisdictional claims in published maps and institutional affiliations.



**Copyright:** © 2021 by the authors. Licensee MDPI, Basel, Switzerland. This article is an open access article distributed under the terms and conditions of the Creative Commons Attribution (CC BY) license (<https://creativecommons.org/licenses/by/4.0/>).

## 1. Introduction

Slope stabilization is probably one of the most typical, ancient and challenging issues of civil engineering. Commonly, problematic landslides affecting buildings and infrastructures are solved by installing a series of measures that lead to completely and immediately stopping the ground movement. Those measures normally include rigid retaining walls, anchors or a substantial variation of the ground profile’s geometry, and their implementation can give rise to a compromise between cost and safety [1–3]. However, when dealing with a great amount of ground material, stopping the movement absolutely and instantaneously may not be the optimal solution. The literature shows the possibility of using different techniques for reducing the mobility of landslides, including small excavations and adjustments of the slope profile, the implementation of flexible walls or piles and the installation of drainage [4–9]. The latter is especially important since landslides are often triggered by precipitations and the resulting change in the groundwater level. Water reduces ground strength and increases pore pressures, contributing to the instability of a slope [7,10–13]. Controlling the water table is essential when dealing with shallow and slow movements, as any rainfall may accelerate or even reactivate a landslide. The previous issues are particularly relevant in areas characterized by rainy seasons followed by dry periods, such as the Mediterranean region and, more precisely, the Iberian Peninsula.

The “El Portalet” Pass is located at the municipality of “Sallent de Gallego”, Huesca province, in Spain, and belongs to the Central Spanish Pyrenees. In 2004, an excavation to

create a parking lot next to a local road was performed in the area. Parking excavation was conducted and resulted in the activation of a large landslide. That landslide occurred on a hillside in the surroundings of Petrusos Peak, in an area of about 0.35 km<sup>2</sup>, where superficial cracking and diverse instabilities at different movement rates had been identified in the past [14]. A carboniferous substrate characterizes the zone, affected by faults of slate nature, with gravel colluvium and sandy clay materials on foothills as a result of previous paleo slides. Natural slopes (average angles of 12°) were also identified to be on the verge of instability [15].

The parking excavation reactivated small slides previously identified in the area [16,17] and produced new ones. The first instability signals were displayed at the end of the year, when large cracks appeared in the head of the slope and propagated afterwards along the hillside, showing cracks and longitudinal and transversal deformations, even breaking the slope toe. This type of deformation characterizes a paleo-slide failure mechanism involving an important volume of material [15,18–20]. Due to the great deformations and large unstable masses involved in the landslide, the typical solutions aimed at absolutely and instantaneously stopping the ground movement would have represented a higher cost than the total elimination of the unstable hillside. Instead, the approach was based on controlling the hillside movement evolution and implementing a series of measures to slow down the ground movements, achieving the stabilization of the slope after some years, but also ensuring no damage to any infrastructure during that time.

This paper shows and analyses the stabilization measures projected and implemented on “El Portalet” Pass. The area has been intensively investigated since 2004 by diverse authors. Classical geotechnical investigations, including boreholes and the installation of inclinometers [15], were conducted after landslide activation. Several Differential GPS campaigns as well as the use of different satellite surface monitoring techniques, including the ground-based SAR (GB-SAR) technique and the Differential Synthetic Aperture Radar Interferometry (DinSAR) technique [14,21–24], were performed from 2006 to 2010. Besides, a new geotechnical investigation was conducted to monitor the landslide evolution 10 years after the initial implementation of the stabilization measures. These data are presented for the first time in this paper. Data coming from all of those investigations are used to assess the performance and the degree of success of the stabilization measures, establishing the expected future evolution of the landslide.

## 2. Materials and Methods

### 2.1. Geographical and Geological Situation

The case study is located at “Sallent de Gallego” (Huesca, Spain). That area belongs to the high basin of the Gallego River Valley (Figure 1), in the Central Spanish Pyrenees.

The studied hillside corresponds with the southwestern slope of the spurs located between Petrusos Peak and the Old Pass of Sallent (latitude 42°48′4.83″ N; longitude 0°24′48.19″ O), with heights between 2128 m and 1848 m. The road next to which the parking lot was built, road A-136, is situated at the hillside foot, and links “El Portalet” Pass and “Sallent de Gallego” village. The Gallego River flows through lower elevations, parallel to the road. The excavation was performed at altitudes between 1735 and 1775 m. Figure 1 shows a parking excavation view, where road A-136 can also be seen.

From the geological point of view, the area under study is located in the Pyrenean Axial Zone, primarily composed of Devonian and Carboniferous materials, amongst which slates (sometimes with sandstone interlayers) are common, with some calcareous zones, all of which are affected by an intense Hercynian folding, accompanied by low-grade metamorphism. From a tectonic point of view, all of these materials are part of the Gavarnie thrust, which contains part of the southern configuration of the Pyrenean chain. Most of the hillside is covered by recent colluvial and quaternary deposits [25–27].

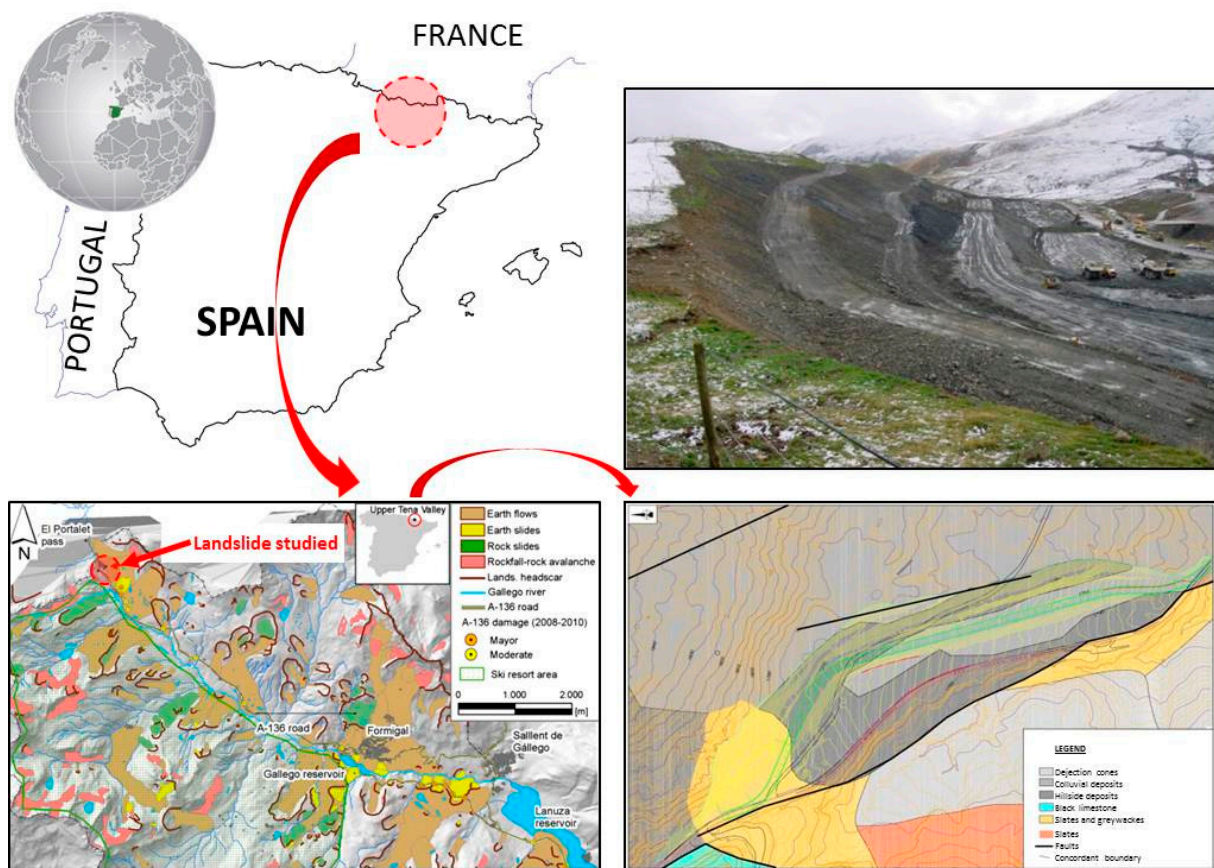


**Figure 1.** Geographical and geological setting of the area under study in the Central Spanish Pyrenees and view of the parking excavation works (note: bottom left image modified from [22]).

The area contains low strength rocks with intense active slope processes and with portions with low structural control. This is observed between the Inner Chains and “El Portalet” on the Gallego River basin, where slates, schists and clays have caused several slope evolution phenomena, associated with mass movements. Slumps are the most spectacular shapes, which leave a scar or tension crack on the head of the slope. Those slumps are deep and affect the substrata, also presenting deep weathering due to both their plasticity and tectonization. In some cases, Devonian slates have acted as a lubricant, their structure and faults located at the top of the slope sometimes causing an additional instability issue. The length of tension cracks can exceed 1 km, and the landslides portray the typical internal corrugation, a consequence of a mass movement.

One of these slumps was mapped by García Ruiz [16,17]. Two parallel tension cracks, which form successive steps (see Figure 1), match the southern slope of the Petrusos spurs and they also overlap with the convex surface presented by the rocky hillside. At its toe, the slumps can be found with two coalescent lobes that reach the fracture northwest of the sunken block of “El Portalet”. The high density of such morphologies can be found on the Gallego head of the slope, especially between “El Portalet” and Formigal ski station in addition to the Peña Foratata southwestern slope, where superposed landslides tend to form great slumps. Most of them do not look very active, but other slumps are still moving or show a local reactivation.

This area is also located in a seismic zone, presenting a basic seismic acceleration of 0.10 g (with g being the gravitational acceleration), according to the Spanish NCSR-02 standard [28].

## 2.2. Previous Field Investigations

Previous geological–geotechnical investigations [15] conducted in 2005 consisted of six boreholes (location is shown in Figure 2) with depths between 24 m and 40 m. Standard Penetration Tests (SPT) were performed on each borehole when crossing soils and very weathered rocks, with a frequency of about 3 m. Disturbed and undisturbed samples were extracted from each level identified. Laboratory tests conducted on such samples included general identification tests (e.g., grain size, Atterberg limits, unit weight) and mechanical tests (uniaxial compression strength on rocks and direct CD shear tests and triaxial CU tests on soils).

Inclinometers were installed on each borehole performed. Besides, topographical landmarks were placed along the hillside to measure surface movements. Attempts to locate landmarks were made next to the existing tension cracks on the head of the slope as well as in the excavated slope. Movements between pairs of landmarks were measured every 15 days and five measurement campaigns were carried out.

In addition, an inventory of water points (e.g., springs and permanent courses) was carried out along the entire hillside, also recording the water table position in the excavated slope.

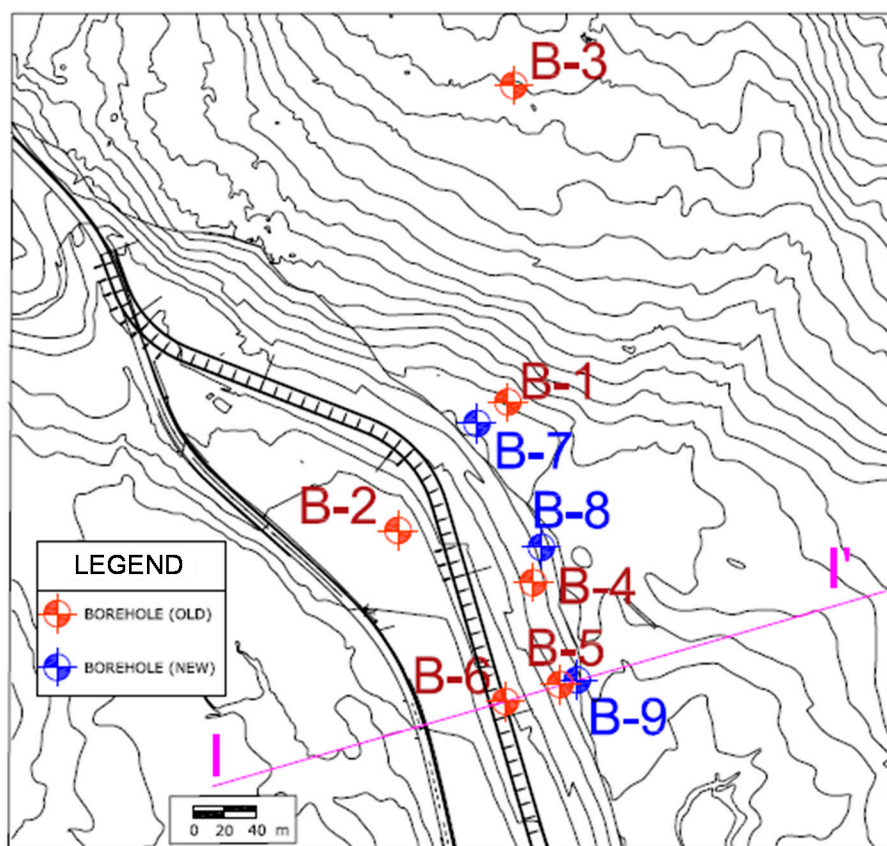


**Figure 2.** Location of the boreholes performed in the previous study [15] (“old” boreholes, conducted in 2005, reprinted with permission from ref. [15], Copyright Year 2005, Copyright Owner’s F.J. Torrijo) and the new geotechnical investigation (“new” boreholes, conducted in 2016); profile I-I’ relates to Figure 5.

## 2.3. Corrective Measures

A series of corrective measures were proposed to be performed on the slope to stabilize the landslide. Those measures (Figure 3) were not aimed to stop the hillside movement immediately and absolutely but to slow it down and prevent any damage to surrounding infrastructures. Eventually, the measures projected were expected to completely stabilize

the hillside and stop the movement (or reduce it to a minimal value) after some years' time. Corrective measures applied included:

- A slight modification of the slope geometry by means of the excavations of intermediate areas (benches) on the slope.
- Installation of deep drainage measures (Californian drains) as well as ditches to improve slope drainage and remove water coming from seepage and runoff; in total, 47 single drains were installed with a separation of 15 m; the horizontal slope was 6% following Serrano and Gómez [29] and Forrester [30]. Drains were executed with slotted PVC pipes with a thickness of 1.5 mm and a diameter of 75 mm.
- Implementation of slope conservation and stabilization measures such as slope profiling and re-vegetation.
- Performance of a flexible retaining wall at the slope toe; wall height was 6 m from the ground and 9.2 m from the bottom of the foundation and its width was found between 3.5 and 4.1 m; its vertical slope was 6:10.

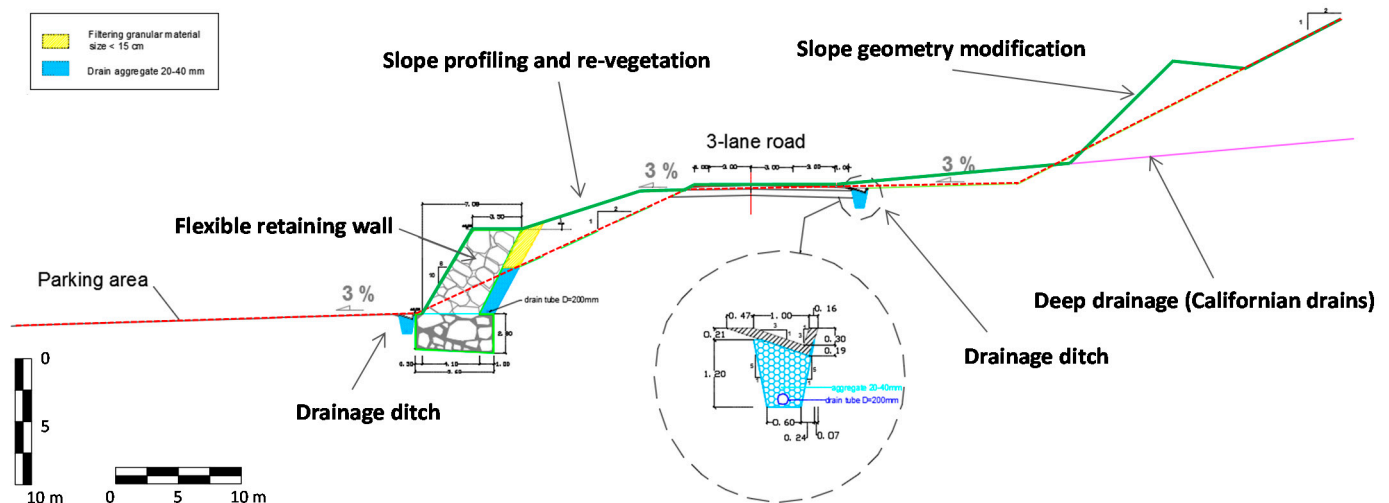


**Figure 3.** Stabilization measures projected; red dotted line and green line show the slope profile before and after implementing the stabilization measures (highlighted in bold), respectively.

#### 2.4. Satellite Surveys

After conducting stabilization works on the slope, the ground-based SAR (GB-SAR) technique was used to monitor the landslide during the years 2006 and 2007 as well as to predict the slope movement evolution [14]. That technique is based on SAR interferometry, i.e., the use of consecutive pairs of SAR images for obtaining information about displacements according to the phase difference (interferogram) between two consecutive SAR images [31,32]. For monitoring the landslide movements [33], the GB-SAR sensor was installed about 600 m from the slope (target distance was between 200 and 1300 m), and worked for 47 days, with an acquisition rate of 1 image per hour, a range resolution of 1.7 m and an azimuth resolution of  $0.74^\circ$ .

Results of GB-SAR were validated with the results of five Differential GPS (DGPS) campaigns, where 93 points were monitored, both stable points located next to the landslide active area and points within the landslide mass. A good match between the two techniques (GB-SAR and DGPS) was found, being the maximum difference 1.5 cm.

In addition, the Differential Synthetic Aperture Radar Interferometry (DinSAR) technique was employed [21,22] to monitor different landslides of the Upper Tena Valley (located in the Central Spanish Pyrenees area), including the area under study. That technique uses microwave remote sensing and produces the measurement of surface displacement of high accuracy with a great coverage capacity [34]. The SPN approach [35],

which combines both the Persistent Scatterers [35–38] and Small Baselines [39–43] methods, was used.

In total, 43 SAR images acquired by ERS-2 and ENVISAT satellites (from 2001 to 2007), 14 SAR images acquired by the TerraSAR-X satellite (2008) and 12 SAR images acquired by ALOS PALSAR (L-band) satellite (from 2006 to 2010) were processed. An auxiliary DGPS campaign was also undertaken to validate the results.

More details about this investigation can be found in [14,21–24].

### 2.5. New Field Investigations

In 2016, approximately 10 years after conducting the stabilization works of the slope, three new boreholes were performed (Figure 4a) at the area under study. Those boreholes attained a depth between 30 m and 45 m and were performed close to those executed in the previous field investigation (see Figure 2). On each borehole, SPT tests were performed in soils and very weathered rocks, with a frequency of about 3 m. Disturbed samples were extracted from each level found and general identification laboratory tests were carried out (grain size, Atterberg limits and unit weight).

Similar to the actions performed in the previous geological–geotechnical investigation, inclinometers were installed on the new boreholes (Figure 4b). Besides, a new inventory of water points was carried out along the entire hillside (Figure 4c).



**Figure 4.** New geotechnical investigation works: (a) Borehole performance; (b) Inclinometer installation; (c) Inventory of water points; (d) Example of the Quaternary material obtained in the boreholes.

### 2.6. Limit Equilibrium Analysis

Stability analysis of the landslide was carried out in its natural state and after implementing the corrective measures based on limit equilibrium methods. These methods consider the static mechanical laws and assume the shear strength of the soil to be totally and simultaneously developed along the sliding surface (failure surface). With such

methods, the slope safety factor may be computed as the ratio between the available shear strength in the sliding surface and the needed shear strength to keep a strict equilibrium of the sliding mass.

Nowadays, the most common way of applying limit equilibrium methods is using the method of slices. This method divides the soil sliding mass into many vertical slices to solve the stability problem. The method assumes that failure of the soil is governed by the Mohr–Coulomb criterion, slices behave as rigid bodies and no stresses exist inside each slice. The equation system obtained once the equilibrium of forces is established on each slice requires assuming different simplifications and/or hypotheses to solve the system, all of which leads to having several “sub-methods”. In this work, Bishop’s method [44] and the Morgenstern–Price method [45] were used. The former is an approximate method that establishes the equilibrium of vertical forces and bending moments, assumes a horizontal resultant of the interslice forces and does not take into account interslice shear forces. The latter is an exact method that establishes the stability problem using the three equilibrium conditions in slices of differential thickness and assumes that the inclination of the forces between slices is proportional to a given function.

Several slope profiles were selected to compute the landslide safety factor applying the two mentioned methods. Simulations were run with and without considering the seismic acceleration (0.10 g, with g being the gravitational acceleration).

### 3. Results

#### 3.1. Field Investigations and Satellite Surveys

In situ (SPT) and laboratory tests conducted on the different investigations carried out identified six geotechnical units in the area under study. Table 1 lists the average parameters of those units related to SUCS classification, Atterberg limits, unit weight, water content and mechanical parameters (cohesion and friction angle for soil materials and uniaxial compression strength for rocks).

**Table 1.** Geotechnical parameters of the materials found in the area under study.

Geotechnical Unit	Depth [m]	SUCS	W <sub>p</sub>	PI	γ [kN/m <sup>3</sup> ]	W [%]	c [kPa]	φ [°]	UCS [MPa]
Colluvial deposits	2–10	GM-GC	30.5	8.4	21.0	7.0	–	29.0	–
Green sand-clay	2–6	SC	32.1	10.4	20.4	14.0	–	18.0	–
Black sand-clay	2–6	SC-GC	30.9	10.6	22.2	8.1	–	25.0	–
Fragmented calcareous rocks and slates	2–6	GC-SC	33.6	12.9	21.7	6.7	–	38.0	–
Fault breccia	–	–	–	–	23.0	6.0	20.0	25.0	–
Slate rock	–	–	–	–	27.7	–	–	–	12.5

Notation: SUCS: Soil Unified Classification System (Casagrande’s classification); W<sub>p</sub>: plastic limit; PI: plasticity index; γ: unit weight; W: water content; c: cohesion (residual); φ: friction angle (residual); UCS: uniaxial compression strength.

Rock mass of the area consisted of variably calcareous slates with calcite filled veins (Geotechnical unit “Slate rock”) belonging to the “Facies Culm” from the Carboniferous period. This rock mass presented an average RQD of 60% and the RMR reached an average value of 60. According to the geological–geotechnical investigations conducted, rocky formation crops out only in the northern area, where no instabilities were detected. The rest of the slope surface is covered by quaternary deposits (Figure 4d), which include colluvial deposits, green clayey sands, black clayey sands and fragmented calcareous rocks and slates. Additionally, fault breccia materials were found in an old fault detected, though currently inactive (yet some water was seen circulating through it). Except for colluvial deposits, quaternary materials come from a roto-translational, with unidirectional movement, landslide that occurred in the area in the past. Materials appeared unstructured and remoulded due to paleo-sliding.

Data from boreholes, inclinometers and surface movements led to defining a failure surface located at depths between 5 m and 19 m (see Figure 5), with a fairly planar shape and with greater curvature in the slope toe area. The failure surface daylights on the slope and is observed on the ground surface (at both the slope head and toe) as seen in Figure 6. Surface movements in the E-SE direction, topographically recorded during the previous geotechnical investigations [15], showed small movements on the head of the slope as well as on the excavated slope. Those movements ranged between 1 cm and 3 cm, with movements in the northern area being slightly inferior to southern areas.

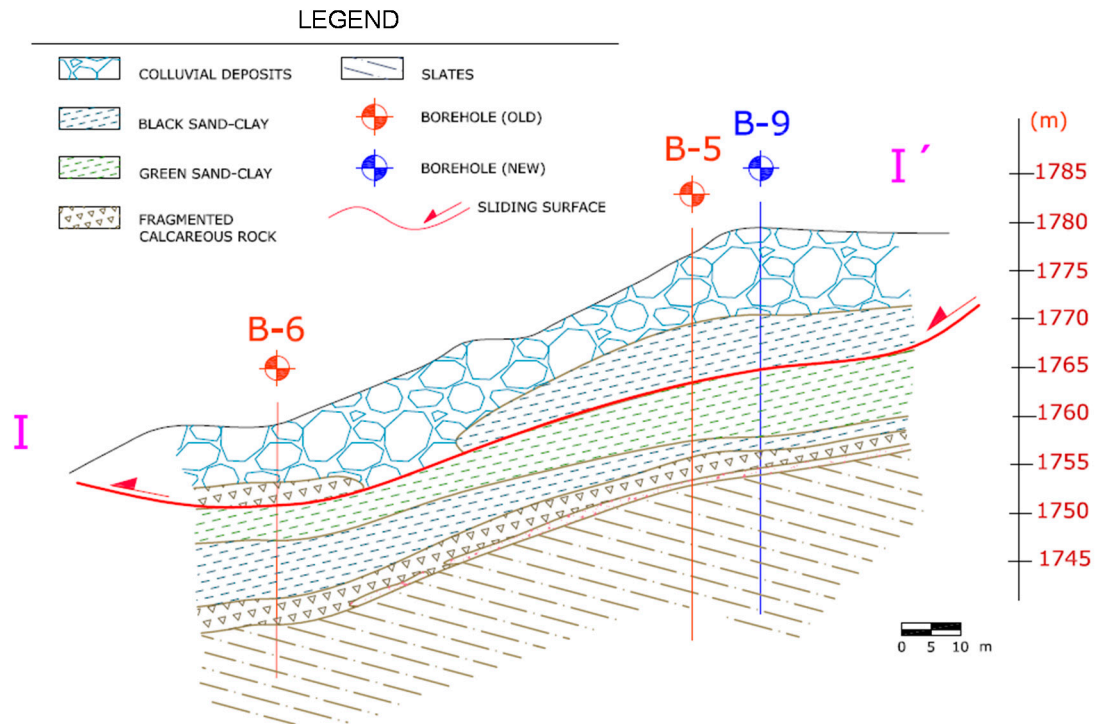


Figure 5. Geotechnical profile I-I' (see Figure 2) of the area under study; failure surface detected is shown in red.

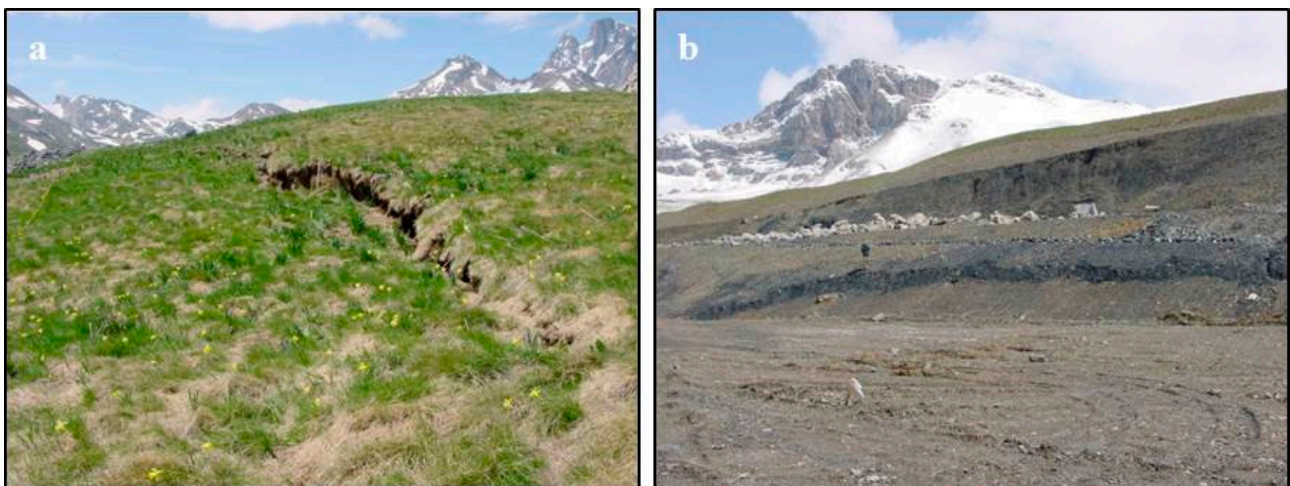
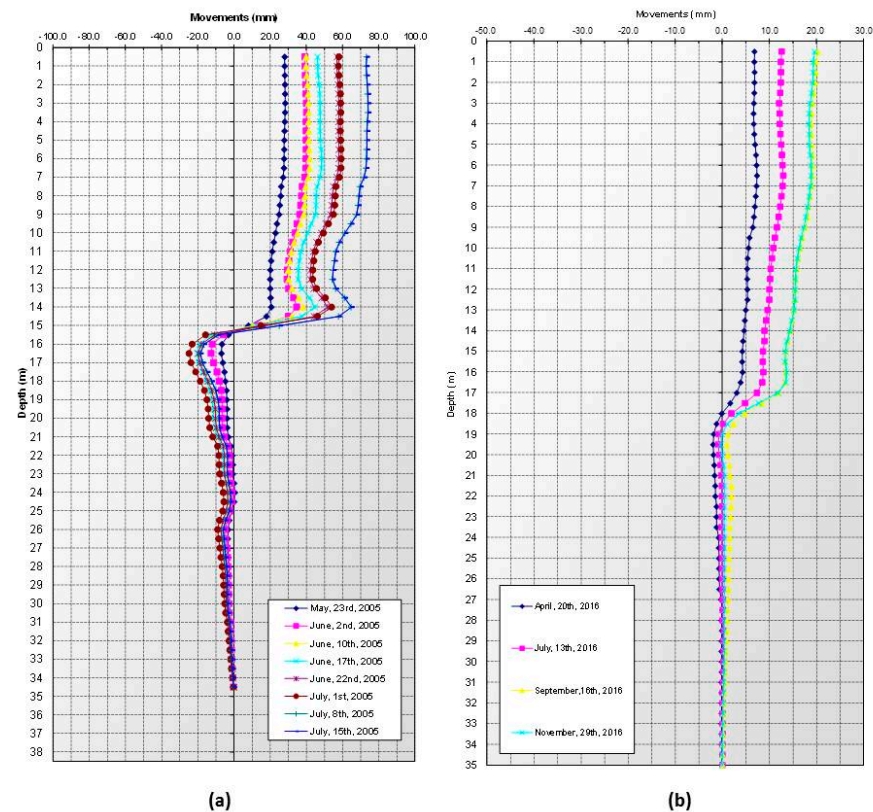


Figure 6. Daylight of the failure surface: (a) stress crack; (b) warped plane morphology.

Inclinometers revealed the development of the failure surface mainly through the sandy clay materials in contact with the fragmented calcareous rock. An example of inclinometer data obtained in the previous study [15] and new geotechnical investigations

is shown in Figure 7 (note that those inclinometers belong to profile I-I' shown in Figure 5; failure surface may be easily identified).



**Figure 7.** Inclinometers records: (a) Inclinometer placed in borehole B-5, reprinted with permission from ref. [15], Copyright Year 2005, Copyright Owner's F.J. Torrijo (old geotechnical investigations [15], conducted in 2005); (b) Inclinometer placed in borehole B-9 (new geotechnical investigations, conducted in 2016).

Topographical works developed during the previous investigation [15] detected the existence of three main landslides in the area under study (landslides, 1, 2 and 3 in Figure 8). This information was confirmed by the DinSAR data [21,22]. One of those landslides (landslide 3) was not affected by any anthropogenic activity (i.e., was not the consequence of the parking excavation) and was an extremely slow movement [46,47] with an estimated average velocity [22] of approximately 16 mm/year and affected by seasonal rainfalls. The second landslide (landslide 1) was activated by the parking excavation and corresponds to the slope movement under study. Its movement rate, estimated by the auxiliary DGPS campaign of approximately 0.1 m/year, meant it was not possible to compute its velocity with the DinSAR technique [22]. The third landslide (landslide 2) was located next to the previous one, was also activated by the parking excavation and its average velocity was estimated [22] at approximately 25 mm/year. The ALOS PALSAR differential interferometry [24] was also applied to this last landslide, obtaining similar results.

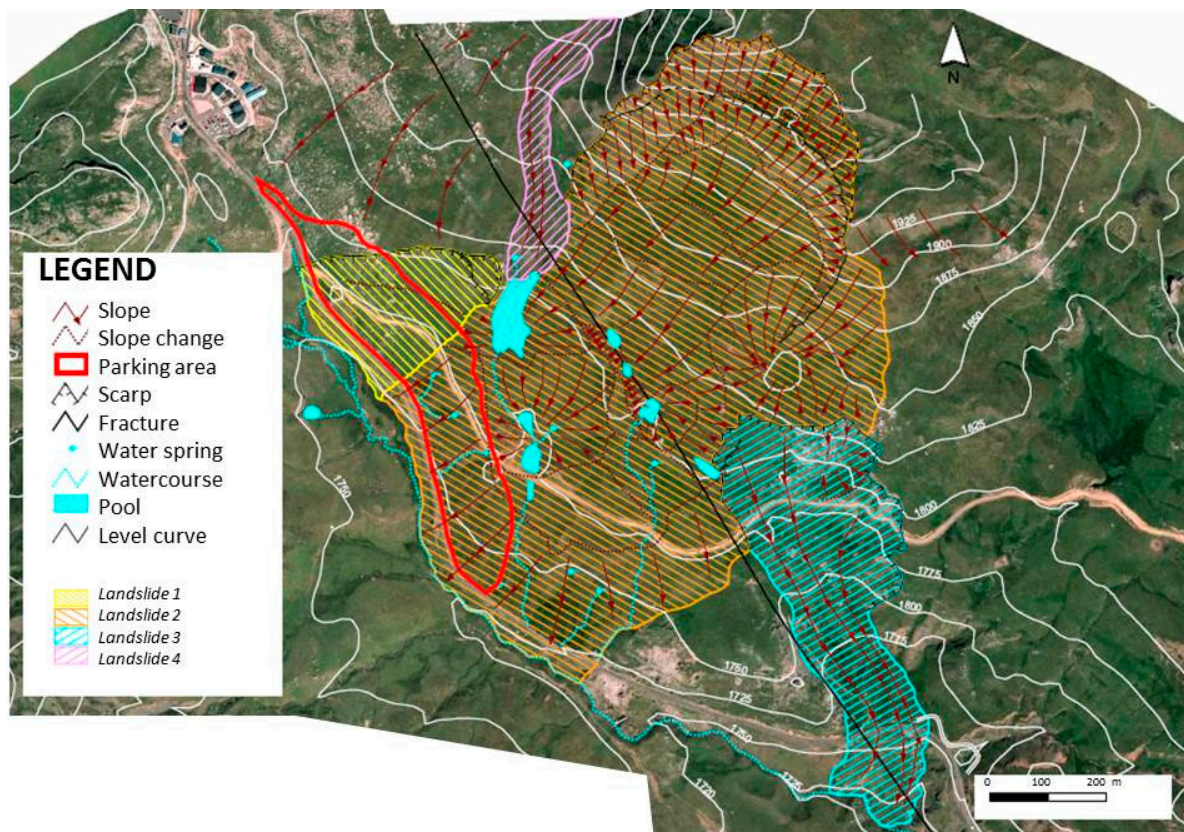


**Figure 8.** Main landslides detected in the area under study.

DGPS measurements [14], conducted after performing the stabilization work on the slope (i.e., landslide 2 according to Figure 8), showed that maximum displacement rates were around 1 mm/day in the summer while rates increased up to 2 mm/day in the fall. Those measurements also identified that the landslide's most active part was an area located below the main scarp. GB-SAR technique discovered that the landslide displacements were fairly linear in time, although slight differences were observed due to daily rainfall variations. Generally, an acceleration of the landslide occurs when rainfall events take place.

In fact, hydrogeological results obtained in the previous study [15] and the new geotechnical investigation indicated that surface materials were permeable and the hillside drains with abundant subterranean water flow. Continuous flow springs near the slope toe were identified, with that flow occurring through both the permeable material and the failure surface. The water table was found approximately on the failure surface, suffering oscillations with precipitations. Thus, the relationship between the landslide evolution rate and rainfall reported by the use of the GB-SAR technique [14] was confirmed due to the easy infiltration of water in the sliding mass, thanks to the high drainage capacity of the colluvial material located on the top of it.

### 3.2. Limit Equilibrium Analysis

Several slope profiles were analysed using limit equilibrium methods by means of the method of slices. The geotechnical parameters obtained in the field investigations and listed in Table 1 were used to conduct such analyses. The Bishop's method [44] was applied to compute the safety factor without considering the seismic action. The Morgenstern–Price method [45] was applied to compute the safety factor considering the seismic action, which was taken into account by a pseudo-static approach considering two orthogonal forces, their value based on the Spanish code [28].

Under natural conditions, once the parking area was excavated and prior to implementing any corrective measure, profile I-I', according to Figures 2 and 5, was found to be the most unfavourable profile. Without taking into account the seismic component, the safety factor at that profile resulted in 0.86. That confirms the existence of the landslide produced by the parking excavation and the subsequent movement of the slope. It should be mentioned that this landslide was a first-time failure, not a reactivation of a previous one. When the seismic action was taken into account, a safety factor of 0.59 was obtained for the same profile (i.e., about 30% lower).

The analyses were run again introducing the projected measures and considering the final stage of the projected slope. The water table was located following the data obtained from the inventory of water points carried out in the new investigations and considering that the capacity of California drains is greater than the recharge of the aquifer (an average level was considered since the water table depends on rainfalls, see the next section). Profile I-I' was still found to be the most unfavourable. In this case, the safety factor without taking into account the seismic component increased to 1.3; taking into account the seismic acceleration, the safety factor was 1.1 (about 15% lower). That result indicates that the slope is stable and the landslide is expected to be under control with the projected measures. Figure 9 shows the results computed by the Bishop's method for profile I-I' before and after implementing the stabilization measures using the software Slide v5.028 [48].

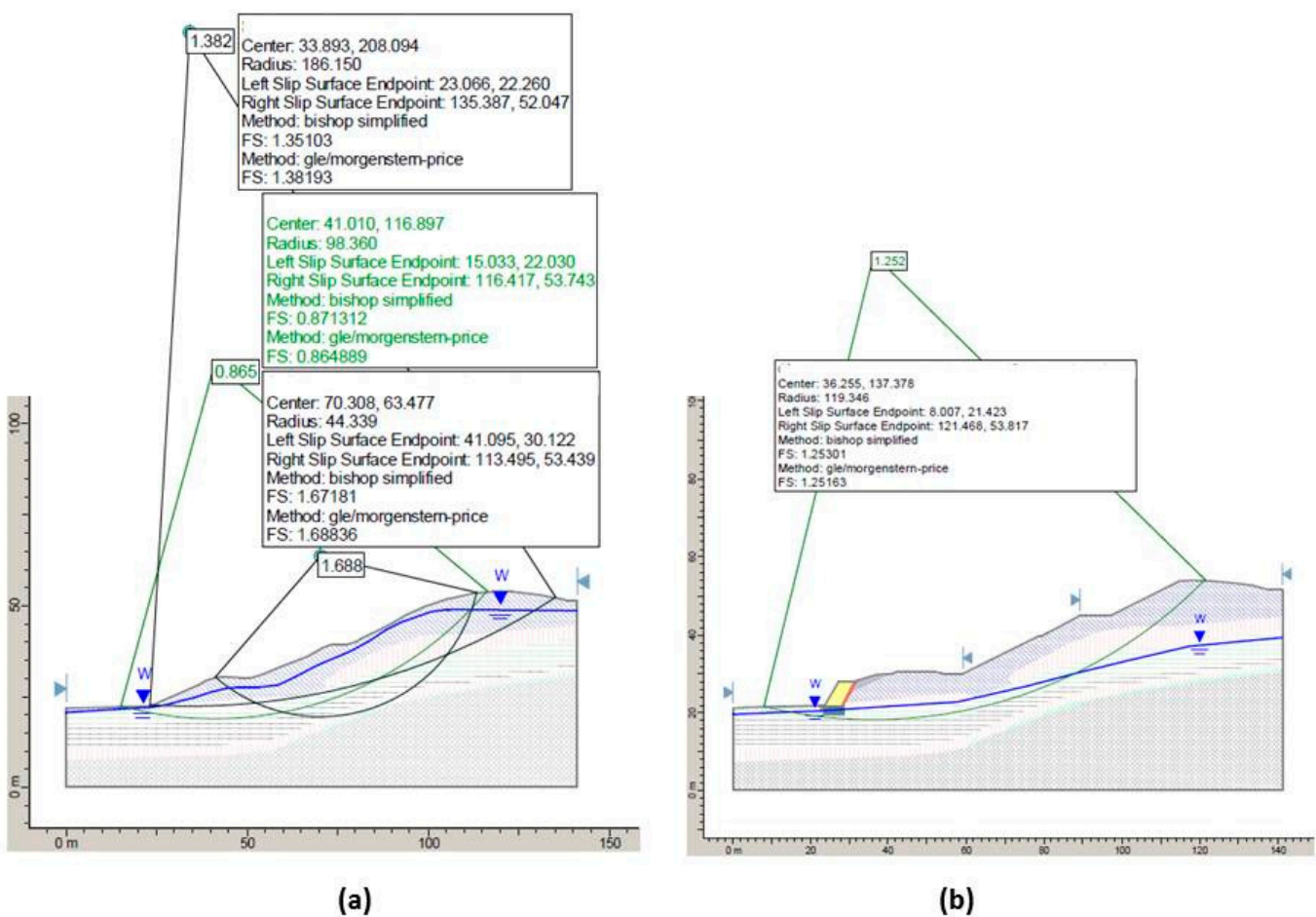


**Figure 9.** Safety factor analyses of profile I-I' (see Figure 2): (a) slope in its natural state after the parking excavation; (b) slope state after implementing the stabilization measures.

It is interesting to mention that the stability analysis calculations conducted considered the whole slope and the corrective measures were designed accordingly. Considering only a part of the slope was not correct, this may have given rise to erroneous results. For

instance, Figure 10 shows a stability analysis carried out by both the Bishop [44] and the Morgenstern–Price [45] methods taking into account only the area around the toe wall. The safety factor obtained was nearly 1.6 in both cases, about 23% and 45%, respectively, greater than that computed in the scenario considered in Figure 9b. This may have led to an assumption that the installation of that wall was the unique corrective measure needed, which resulted in it not being enough for controlling the hillside movement.

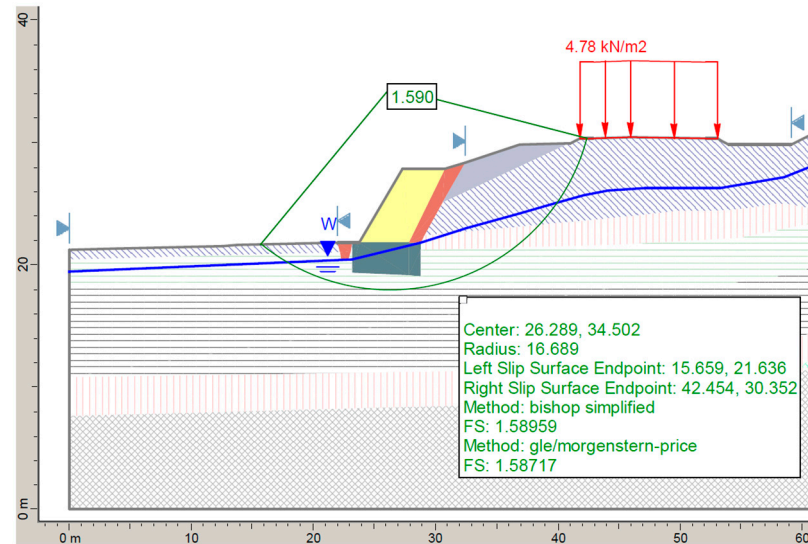


**Figure 10.** Stability analysis considering the projected wall alone.

### 3.3. Drainage Evolution

Water table lowering plays an essential role in the stability of the landslide studied. The approximate volume of the adjacent aquifer to the area under study was estimated at  $0.86 \text{ Hm}^3$ . However, based on the available data, the aquifer lateral supply was unknown, so this volume could be much higher. Although the effective porosity of the different materials traversed by the Californian drains was also unknown, adopting an estimated value of 5–7%, the volume of water to drain is probably between  $100,000 \text{ m}^3$  and  $200,000 \text{ m}^3$ . Besides, the groundwater recharge of the aquifer should be considered and this does not stop, being especially significant due to the high rainfalls in the area. Recharge can be estimated at around 1900 mm per year, widely distributed throughout the year except for the summer season.

As a consequence, the water table lowering does not only depend on the drainage capacity and the efficiency of the Californian drain but also on the weather and the annual recharge (Figure 11). As a result, the drainage of the slope needs time. During that time, the slope is expected to have a safety factor lower than 1.0, which explains the movement of the slope recorded by the different investigations (in fact, the safety factor increased from the situation depicted in Figure 9a to the one given in Figure 9b). Thus, although the future solution in the long term will be stable, attaining this situation will need to wait for some time during which the slope will exhibit unstable behaviour.

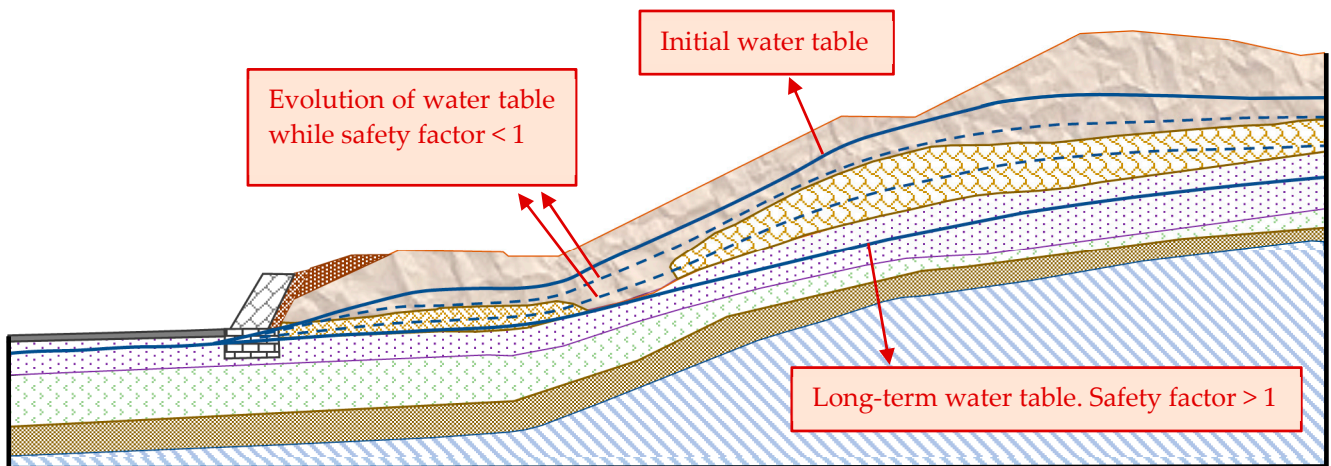


Figure 11. Expected evolution of the water table and its qualitative relationship with the safety factor.

Although the tendency of the water table is the one explained, this evolution does not take place through a uniform decay. Figure 12 shows the evolution of the lateral displacements recorded by the inclinometers located at a depth of 5 m in boreholes B5 and B9 (Figure 7). Both boreholes were located close to one another and correspond to the previous (year 2005) and new (year 2016) geotechnical investigations, respectively.

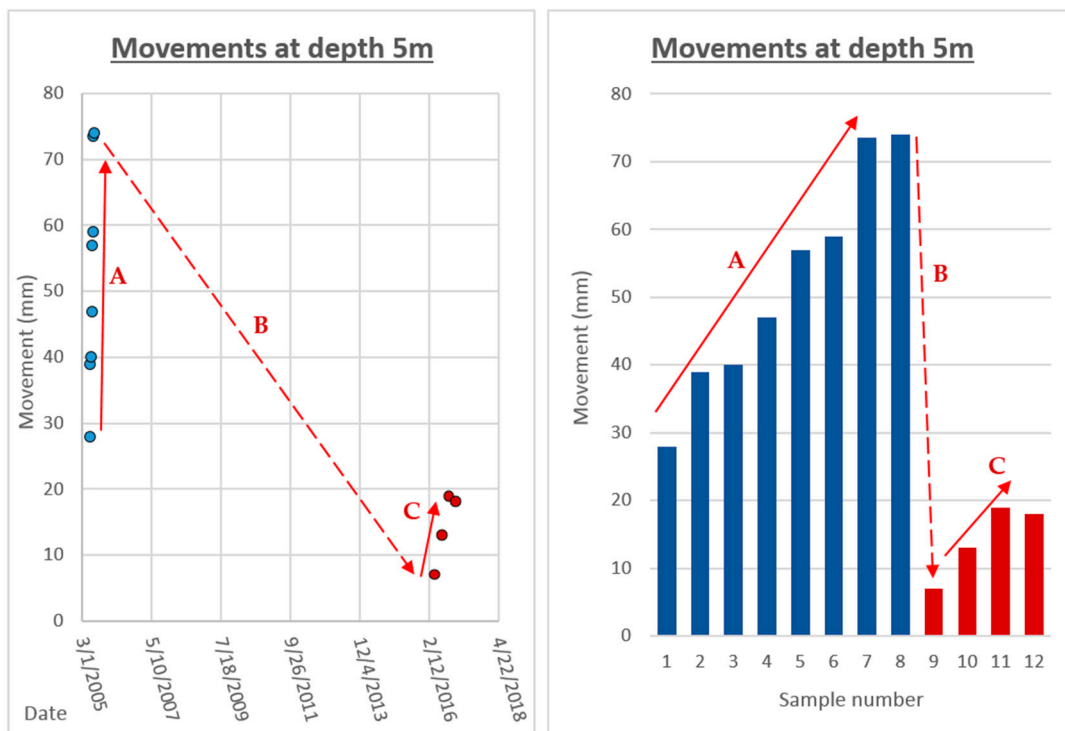


Figure 12. Evolution of the movements at a depth of 5 m. Long-term trend. The movements are represented in blue for borehole B5 (installed in year 2005) and brown for borehole B9 (installed in year 2016), Date given in Day/Month/Year. Letter A refers to the fast increment in deformations in 2005; B refers to the reduction of deformations between 2005 and 2016; C refers to the acceleration of deformations registered in 2016.

Figure 12 shows that, in 2005, the deformations were increasing and the slope was moving faster (A). Between 2005 and 2016 the deformations were greatly reduced, so the landslide was stopping (B). Finally, according to 2016 records, the slope continued to accelerate; from April to September the movement evolved from 5 to 20 mm, although from

September to November it seemed to stabilize (C). This acceleration in a given year was also observed in 2005 for the same period, April to September. That period corresponds to the spring season when precipitations normally occur in the area under study together with the snowmelt phenomenon [49]. Thus, these results confirm the influence of the water table in the landslide stability, the long-term tendency observed in the evolution of the slope movement and the long time needed to attain drainage of the ground mass (Supplementary Materials).

#### 4. Discussion

The case study presented in this paper at “El Portalet” Pass in the Spanish Pyrenees is an example of dealing with a large landslide by slowing it and controlling its behaviour by different instrumentation and monitoring techniques. The proposed approach was fostered by the slow surface movements (about 0.3 m/year) observed during the previous geotechnical investigations and recorded in the inclinometers installed [15]. This value led to the conclusion that the hillside material had a slow type of movement [46] with both distensile and compressive areas. Therefore, permanent infrastructures (such as the parking lot) situated over the hillside were expected not to be seriously harmed by the natural movement of the slope. Nevertheless, stability of the landslide in the long term must be ensured due to both safety and economic efficiency of the parking lot and the surrounding area.

The slow movement allowed for the projection of a series of hillside stabilization measures that tended towards the reduction of the movement rate velocity, which eventually attained the total stopping of the landslide evolution. These measures included the modification of the slope geometry, the installation of drainage and the construction of a flexible retaining toe wall. Data obtained from diverse geotechnical investigations, satellite monitoring [14,15,18,19,21–24] and numerical models were used to assess the effectiveness of such measures. In addition, new geotechnical investigations, involving new boreholes and the installation of new inclinometers, were conducted, showing that the evolution of the landslide tends towards its total stabilization (no movement).

The initial design of the parking lot included a basic stability analysis of the hillside and the implementation of a rigid retaining wall to contain the ground [15]. The landslides activated once the parking area was excavated however, which showed an inefficacy of the analysis and measures. As indicated in Section 3.2, the stability analysis of the area under study should have considered the entire slope and not have been restricted to the area just adjacent to the parking excavation to avoid erroneous results and misunderstand the measures needed. A stability analysis that leads to a safety factor greater than 1.0 does not guarantee the slope to be stable, especially when involving large areas, as is the case under study. Besides, it should be noted that limit equilibrium methods do not consider deformations, so a slope may be unstable sometimes even though the safety factor is greater than 1.0, as reported in some cases found in the literature [50].

An important aspect involving a large area and also shown in this case study is the possibility that a landslide triggers other landslides in the area. The cascade effect that a potential landslide may have in other points of the slope should never be neglected. These additional landslides are difficult to predict unless a geological exploration is conducted in the area potentially affected. All in all, the stability analysis of potential landslides involving large ground masses, even though adjusted to the corresponding design requirements, should be supported on thorough geological and geotechnical surveys that enable an assessment that the analysis conducted properly fits the natural processes.

In the case under study, the influence of the water table plays a critical role in the stability of the landslide. In particular, the drainage time needed for lowering the water table was shown to be decisive in the instability of the system. Thus, establishing only a future situation and assuming this situation will be reached in a short term may give rise to errors. As shown in this work, stability takes time to be reached, an issue that should be considered in the design of slope stability measures and the subsequent monitoring

process. Thus, although a large number of drains were installed, the water outlet from the aquifer did not have a high discharge ratio, so lowering the water table needs more than 10 years to be effective.

Regional climatology showed a direct influence on the water table evolution. The region under study presents high values of rain and snow precipitation as well as snowmelt events [49], all of which prevent the water table from decreasing efficiently. According to the data obtained by the inclinometers installed at the geotechnical investigations, during certain periods of the year the water table increases, as indicated by the landslide acceleration in 2016. This result is evidence that the water table does not always decrease but it may also increase in some periods throughout the year in which the water supply (due to precipitation and snowmelt events) exceeds the outlet of water through the drainage measures.

Therefore, the transition period between the construction works and the stabilization of the long-term water table may give rise to an unfavourable scenario in terms of stability. This motivates the need for monitoring of large landslides such as this case under study to establish the moment when the landslide may be considered to be under control. In this case under study, once the water table reaches the desired level considered in the stability analyses, seasonal oscillations are not expected to cause any instability in the slope, so the landslide may be considered stable and no significant movements of the ground are expected from that point.

Finally, it is interesting to mention that the cost of the stabilization measures carried out in this case study is estimated at EUR 1.5 M. This type of solution forces slope control (monitoring) and the acceptance of a certain degree of ground deformations, however, considering that the cost of the implementation of the common measures aimed to totally stop the landslide would be considerably much higher, it is clear that the engineering solution adopted was a good answer for solving the classical engineering duality cost–safety.

**Supplementary Materials:** A Kmz file is available at <https://www.mdpi.com/article/10.3390/app11167176/s1>.

**Author Contributions:** Conceptualization, F.J.T. and J.G.-R.; methodology, F.J.T. and J.G.-R.; project administration, G.C. and F.J.T.; software, J.G.-R.; validation, G.C. and F.J.T.; formal analysis, M.Á.E. and F.J.T.; writing—original draft preparation, J.G.-R.; writing—review and editing, G.C. and M.Á.E.; visualization, G.C. and M.Á.E.; supervision, G.C. and F.J.T. All authors have read and agreed to the published version of the manuscript.

**Funding:** This research did not receive any specific grant from funding agencies in the public, commercial, or not-for-profit sectors. The authors fully acknowledge the financial support provided by the Department of Geological and Geotechnical Engineering of the UPV.

**Institutional Review Board Statement:** Not applicable.

**Informed Consent Statement:** Not applicable.

**Data Availability Statement:** The data presented in this study are available on request from the corresponding author. The data are not publicly available due to privacy reasons.

**Acknowledgments:** Authors thank ICOG for providing them with the geotechnical data related to the “previous geotechnical investigation” works. Thanks are also given to IBERGEOTECNIA for its collaboration in the “new geotechnical investigation” works.

**Conflicts of Interest:** The authors declare no conflict of interest.

## References

1. González de Vallejo, L.I.; Beltrán, F.J.; Ferrer, M. Estabilización y control de un gran deslizamiento en rocas lutíticas. In Proceedings of the III National Symposium on Slopes and Unstable Hillsides, La Coruña, Spain, 3 December 1992.
2. Jiang, Q.; Qi, Z.; Wei, W.; Zhou, C. Stability assessment of a high rock slope by strength reduction finite element method. *Bull. Eng. Geol. Environ.* **2014**, *74*, 1153–1162. [[CrossRef](#)]
3. Moreno, J.; Peña, A.; Pinto, H. Dynamic Barriers for Protections against Rocks Falls. *Rev. Construcción* **2016**, *15*, 27–37. [[CrossRef](#)]

4. Hutchinson, N.N. Assessment of the effectiveness of corrective measures in relation to geological conditions and types of slope movement. *Bull. Int. Assoc. Eng. Geol.* **1977**, *16*, 131–155. [[CrossRef](#)]
5. D'Acunto, B.; Urciuoli, G. Groundwater regime in a slope stabilized by drain trenches. *Math. Comput. Model* **2006**, *43*, 754–765. [[CrossRef](#)]
6. Cotecchia, F.; Lollino, P.; Petti, R. Efficacy of drainage trenches to stabilise deep slow landslides. *Geotech. Lett.* **2016**, *6*, 1–6. [[CrossRef](#)]
7. Conte, E.; Troncone, A. A performance-based method for the design of drainage trenches used to stabilize slopes. *Eng. Geol.* **2018**, *239*, 158–166. [[CrossRef](#)]
8. Wei, Z.L.; Wang, D.F.; Xu, H.D.; Sun, H.Y. Clarifying the effectiveness of drainage tunnels in landslide controls based on high-frequency in-site monitoring. *Bull. Eng. Geol. Environ.* **2020**, *79*, 3289–3305. [[CrossRef](#)]
9. Troncone, A.; Pugliese, L.; Lamanna, G.; Conte, E. Prediction of rainfall-induced landslide movements in the presence of stabilizing piles. *Eng. Geol.* **2021**, *288*, 106143. [[CrossRef](#)]
10. Wei, Z.L.; Lü, Q.; Sun, H.Y.; Shang, Y.Q. Estimating the rainfall threshold of a deep-seated landslide by integrating models for predicting the groundwater level and stability analysis of the slope. *Eng. Geol.* **2019**, *253*, 14–26. [[CrossRef](#)]
11. Zhi, M.M.; Shang, Y.Q.; Zhao, Y.; Lü, Q.; Sun, H.Y. Investigation and monitoring on a rainfall-induced deep-seated landslide. *Arab. J. Geosci.* **2016**, *9*, 182. [[CrossRef](#)]
12. Corominas, J.; Moya, J.; Ledesma, A.; Lloret, A.; Gili, J.A. Prediction of ground displacements and velocities from groundwater level changes at the Vallcebre landslide (eastern Pyrenees, Spain). *Landslides* **2005**, *2*, 83–96. [[CrossRef](#)]
13. Rosone, M.; Ziccarelli, M.; Ferrari, A.; Camillo, A. On the reactivation of a large landslide induced by rainfall in highly fissured clays. *Eng. Geol.* **2018**, *235*, 20–38. [[CrossRef](#)]
14. Herrera, G.; Fernández-Merodo, J.A.; Mulas, J.; Pastor, M.; Luzi, G.; Monserrat, O. A landslide forecasting model using ground based SAR data: The Portalet case study. *Eng. Geol.* **2009**, *105*, 220–230. [[CrossRef](#)]
15. Torrijo, F.J.; Sarasa, A. *Informe Sobre las Inestabilidades Detectadas en Una Ladera en las Inmediaciones del Puerto de Portalet (Sallent de Gállego, Huesca), Donde se Está Ejecutando la Construcción de un Futuro Aparcamiento*; Technical Report; Zaragoza Ilustre Colegio Oficial de Geólogos de Aragón (ICOG): Zaragoza, Spain, 2005.
16. García Ruiz, J.M. *Mapa Geomorfológico de Sallent (Huesca) a Escala 1:50,000*; Geoforma Ediciones: Logroño, Spain, 1999.
17. García Ruiz, J.M.; Chueca, J.; Julián, A. Los movimientos en masa del alto Gállego. In *Geografía Física de Aragón. Aspectos Generales y Temáticos*; Peña, J.L., Longares, L.A., Sánchez, M., Eds.; Universidad de Zaragoza e Institución Fernando el Católico: Zaragoza, Spain, 2004; pp. 141–152.
18. Torrijo, F.J.; Andrés, J.; Sarasa, A.; Bona, M.E. Estudio y propuesta de corrección de las inestabilidades detectadas en la zona de “El Portalet” (Huesca). In *Proceedings of the VII National Symposium on Slopes and Unstable Hillsides*, Barcelona, Spain, 27–30 October 2009.
19. Torrijo, F.J.; Rodrigo, M.; Esteban, C. Instrumentación y corrección de las inestabilidades detectadas en la zona de “El Portalet” (Huesca, España). In *Proceedings of the VIII Chile Conference on Geotechnical Engineering*, Santiago, Chile, 26–29 November 2014.
20. Chistaras, B.; Argyriadis, M.; Moraiti, E. Landslides in the marly slope of the Kapsali area in Kithira Island, Greece. *Bull. Eng. Geol. Environ.* **2014**, *73*, 839–844. [[CrossRef](#)]
21. Herrera, G.; Notti, D.; García-Davalillo, J.C.; Mora, O.; Cooksley, G.; Sánchez, O. Analysis with C-and X-band satellite SAR data of the Portalet landslide area. *Landslides* **2011**, *8*, 195–206. [[CrossRef](#)]
22. Herrera, G.; Gutiérrez, F.; García-Davalillo, J.C.; Guerrero, J.; Notti, D.; Galve, J.P.; Fernández-Merodo, J.A.; Cooksley, G. Multi-sensor advanced DInSAR monitoring of very slow landslides: The Tena Valley case study (Central Spanish Pyrenees). *Remote Sens. Environ.* **2013**, *128*, 31–43. [[CrossRef](#)]
23. Notti, D.; García-Davalillo, J.C.; Herrera, G.; Mora, O. Assessment of the performance of X-band satellite radar data for landslide mapping and monitoring: Upper Tena Valley case study. *Nat. Hazards Earth Syst. Sci.* **2010**, *10*, 1865–1875. [[CrossRef](#)]
24. García-Davalillo, J.C.; Herrera, G.; Notti, D.; Strozzi, T.; Álvarez-Fernández, I. DInSAR analysis of ALOS PALSAR images for the assessment of very slow landslides: The Tena Valley case study. *Landslides* **2014**, *11*, 225–246. [[CrossRef](#)]
25. Galé, C. *Evolución Geoquímica, Petrográfica y de Condiciones Geodinámicas de los Magmatismos Pérmicos en los Sectores Central y Occidental del Pirineo*. Ph.D. Thesis, Universidad de Zaragoza, Zaragoza, Spain, 2005.
26. Herrero, L. *Caracterización de Inestabilidades de Ladera y Propuesta de Actuación en Sallent de Gállego*. Master's Thesis, Universitat Politècnica de València, Valencia, Spain, 2010.
27. I.T.G.E. *Mapa Geológico de España a Escala 1:50,000*; Hoja 145; Sallent: Madrid, Spain, 1990; p. 54, 1 mapa.
28. NCSR-02. *Seismic Resistance Construction Standard*; Spanish Ministry of Public Works: Madrid, Spain, 2002.
29. Serrano, P.A.; Gómez, R. Métodos de estabilización de taludes en suelos. In *Manual de Estabilización y Revegetación de Taludes*; López Jimeno, C., Ed.; U.D. Proyectos, E.T.S.I. Minas, Universidad Politécnica de Madrid: Madrid, Spain, 1999; pp. 151–244.
30. Forrester, K. *Subsurface Drainage for Slope Stabilization*; ASCE Press: Reston, VA, USA, 2000; p. 208.
31. Bamler, R.; Hartl, P. Synthetic aperture radar interferometry. *Inverse. Probl.* **1998**, *14*, R1–R154. [[CrossRef](#)]
32. Noferini, L.; Pieraccini, M.; Mecatti, D.; Macaluso, G.; Atzeni, C.; Mantovani, M.; Marcato, G.; Pasuto, A.; Silvano, S.; Tagliavini, F. Using GB-SAR technique to monitor slow moving landslide. *Eng. Geol.* **2007**, *95*, 88–98. [[CrossRef](#)]

33. Tarchi, D.; Casagli, N.; Fanti, R.; Leva, D.D.; Luzi, G.; Pasuto, A.; Pieraccini, M.; Silvano, S. Landslide monitoring by using ground-based SAR interferometry: An example of application to the Tessina landslide in Italy. *Eng. Geol.* **2003**, *68*, 15–30. [[CrossRef](#)]
34. Rosen, P.A.; Hensley, S.; Joughin, I.R.; Li, F.K.; Madsen, S.N.; Rodríguez, E. Synthetic aperture radar interferometry. *Proc. IEEE* **2000**, *88*, 333–382. [[CrossRef](#)]
35. Arnaud, A.; Adam, N.; Hanssen, R.; Inglada, J.; Duro, J.; Closa, J. ASAR ERS interferometric phase continuity. In Proceedings of the IGARSS 2003, Toulouse, France, 21–25 July 2003.
36. Ferretti, A.; Prati, C.; Rocca, F. Permanent scatterers in SAR interferometry. *IEEE Trans. Geosci. Remote* **2001**, *39*, 8–20. [[CrossRef](#)]
37. Hooper, A.; Zebker, H.; Segall, P.; Kampes, B. A new method for measuring deformation on volcanoes and other natural terrains using InSAR persistent scatterers. *Geophys. Res. Lett.* **2004**, *31*, 23. [[CrossRef](#)]
38. Werner, C.; Wegmüller, U.; Strozzi, T.; Wiesmann, A. Interferometric point target analysis for deformation mapping. In Proceedings of the IGARSS 2003, Toulouse, France, 21–25 July 2003.
39. Berardino, P.; Fornaro, G.; Lanari, R.; Sansosti, E. A new algorithm for surface deformation monitoring based on small baseline differential SAR interferograms. *IEEE Trans. Geosci. Remote* **2002**, *40*, 2375–2383. [[CrossRef](#)]
40. Lundgren, P.; Casu, F.; Manzo, M.; Pepe, A.; Berardino, P.; Sansosti, E. Gravity and magma induced spreading of Mount Etna volcano revealed by satellite radar interferometry. *Geophys. Res. Lett.* **2004**, *31*, L04602. [[CrossRef](#)]
41. Mora, O.; Mallorquí, J.J.; Broquetas, A. Linear and nonlinear terrain deformation maps from a reduced set of interferometric SAR images. *IEEE Trans. Geosci. Remote* **2003**, *41*, 2243–2253. [[CrossRef](#)]
42. Prati, C.; Ferretti, A.; Perissin, D. Recent advances on surface ground deformation measurement by means of repeated spaceborne SAR observations. *J. Geodyn.* **2010**, *49*, 161–170. [[CrossRef](#)]
43. Schmidt, D.A.; Bürgmann, R. Time-dependent land uplift and subsidence in the Santa Clara Valley, California, from a large interferometric synthetic aperture radar data set. *J. Geophys. Res. Atmos.* **2003**, *108*, 2416. [[CrossRef](#)]
44. Bishop, A.W. The use of slip circle in the stability analysis of slopes. *Geotechnique* **1955**, *5*, 7–17. [[CrossRef](#)]
45. Morgenstern, N.R.; Price, V. The analysis of the stability of general slip surfaces. *Geotechnique* **1965**, *15*, 79–93. [[CrossRef](#)]
46. Cruden, D.M.; Varnes, J. Landslide types and processes. In *Landslides Investigation and Mitigation Special Report 247*; Turner, K., Schuster, R., Eds.; Transportation Research Board: Washington, DC, USA, 1996; pp. 36–90.
47. Glade, T.; Crozier, M.J. The nature of landslide hazard impact. In *Landslide Hazard and Risk*; Glade, T., Anderson, M., Crozier, M.J., Eds.; Wiley: Chichester, UK, 2005; pp. 43–74.
48. RocScience. *Slide Manual*; RocScience, Inc.: Toronto, ON, Canada, 2005.
49. Lastrada, E.; Garzón-Roca, J.; Cobos, G.; Torrijo, F.J. A Decrease in the Regulatory Effect of Snow-Related Phenomena in Spanish Mountain Areas Due to Climate Change. *Water* **2021**, *13*, 1550. [[CrossRef](#)]
50. Garzón-Roca, J.; Torrijo, F.J.; Company, J.; Capa, V. Designing Soil-Nailed Walls Using the Amherst Wall Considering Problematic Issues during Execution and Service Life. *Int. J. Geomech. ASCE* **2019**, *19*, 05019006. [[CrossRef](#)]